Tensile Properties of Smooth Muscle Cells, Elastin, and Collagen Fibers

7

Takeo Matsumoto, Shukei Sugita, and Kazuaki Nagayama

Abstract

Artery walls change their dimensions as well as mechanical properties adaptively in response to mechanical stimulation. Because these responses are caused by the vascular smooth muscle cells (VSMCs) in the media, detailed understanding of the mechanical environment of the VSMCs is indispensable to know the mechanism of the adaptation. Artery wall has been often assumed to be homogenous in conventional mechanical analyses from macroscopic viewpoint. At a microscopic level, however, it is highly heterogeneous, and conventional mechanical analyses using homogeneous models are far from satisfactory to estimate the mechanical environment of the VSMCs. Thus, the mechanical properties of each element composing the artery wall, i.e., VSMCs, elastin, and collagen fibers, should be measured directly. In this chapter, we first introduce the experimental techniques used for the tensile testing of tissues and cell at a microscopic scale and review the tensile properties of VSMCs in detail, and then, those of elastin and collagen fibers. In contrast to elastin and collagen fibers that are simple passive materials, VSMCs are alive and their mechanical properties are highly complicated. Their mechanical properties are reviewed from the viewpoints of smooth muscle contraction, anisotropy in cytoskeletal structure, and viscoelasticity.

Keywords

Anisotropy • Contraction • Relaxation • Tensile test • Viscoelasticity

T. Matsumoto (✉) • S. Sugita • K. Nagayama
Department of Mechanical Engineering, Biomechanics Laboratory, Nagoya Institute of Technology, Gokiso-cho, Showa-ku, Nagoya 466-8555, Japan
e-mail: takeo@nitech.ac.jp

K. Tanishita, K. Yamamoto (eds.), *Vascular Engineering*,
DOI 10.1007/978-4-431-54801-0_7

7.1 Microscopic Tensile Test of the Components in the Vascular Tissues

7.1.1 Needs for Tensile Test

Artery wall has been often assumed to be homogenous in conventional mechanical analyses from macroscopic viewpoint. At a microscopic level, however, it is highly heterogeneous. For example, the medial wall of elastic arteries has a layered structure called a lamellar unit, a pair of elastic lamina mainly composed of elastin and a smooth muscle-rich layer mainly composed of VSMCs and collagen (Wolinsky and Glagov 1967), and Young's modulus of elastin, VSMCs, and collagen is about 0.6 MPa (Fung 1981), 10–100 kPa (Matsumoto and Nagayama 2012), and 1 GPa (Fung 1981), respectively. Thus, it is very important to know the mechanical behavior of these components in detail to know the intramural mechanical environment at a microscopic level. Since artery walls stretched by 30–50 % both in the circumferential and longitudinal directions in the physiological state with reference to no load condition, the mechanical properties of the elements in the artery wall under large deformation are indispensable. Conventional methodology used for the measurement of the mechanical properties of cells such as micropipette aspiration (Hochmuth 2000), magnetic particle twisting (Wang et al. 1993), and nanoindentation with atomic force microscopy (AFM) (Hoh and Schoenenberger 1994; Sato et al. 2000) can only provide the mechanical properties of local regions of cells under small deformation and it is not appropriate for the microscopic mechanical analysis of the artery wall. We, therefore, need to develop another method that can be used to measure the mechanical properties under large deformation. For this purpose, tensile test is useful (Matsumoto and Nagayama 2012).

7.1.2 Tensile Tester

Figure 7.1 shows an example of tensile tester developed in our laboratory for microscopic specimens (Nagayama and Matsumoto 2008). The specimen was observed with an inverted microscope (TE2000E, Nikon Japan), and both ends of the specimen were gripped with two glass micropipettes, an operation pipette and a deflection pipette, with tip diameters of approximately 5–8 μm. There are several methods for specimen gripping. If the specimen is long enough (several 100 mm), it can be gripped by knotting each end around a micropipette tip (Warshaw and Fay 1983). For a shorter specimen, one can grip it by aspirating it at both ends into micropipettes, or by gently pressing the micropipettes, microrods, or microplates onto its lateral surface. Since the specimen is stretched at a portion of their surface in the latter method, shear deformation might appear in the specimen. However, the stiffness obtained in the two methods has been reported to be similar (Nagayama et al. 2006). The surface of the microtools is often coated with various adhesives, such as a cellular adhesive (Cell-Tak, Becton Dickinson, USA) and a urethane adhesive (Polycel, Macklanburg-Duncan, USA), to improve the adhesion.

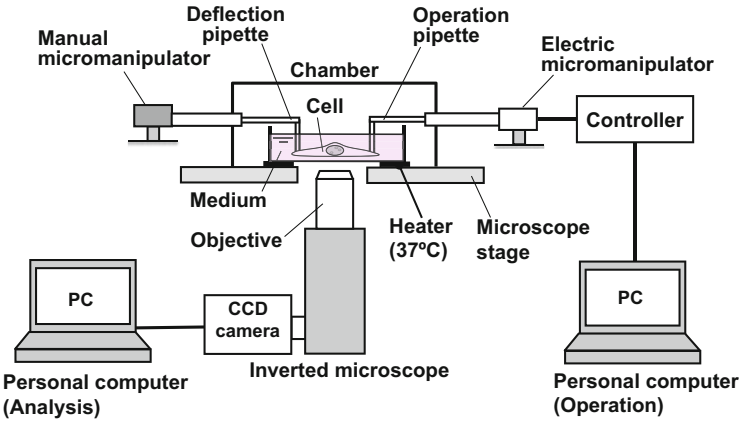

Fig. 7.1 An example of a micro tensile tester

The operation pipette was then moved with a computer-controlled electrical manipulator (MMS-77, Shimadzu, Japan) to stretch the cell horizontally. The force applied to the cell was measured by the deflection of a cantilever part of a deflection pipette that was calibrated after each test. The cell stretching process was observed with a CCD camera (ORCA-ER, Hamamatsu Photonics, Japan) connected to the microscope for an off-line analysis performed later. Spatial resolution of the images taken into the computer was 0.18 μm. Spring constant of the cantilever was 0.006–0.182 N/m, and thus the force resolution was smaller than 0.1 μN.

7.1.3 Data Analyses

After mechanical test, recorded images were fed to a computer to measure the positions of the pipette tips with image analysis software ImageJ (NIH, USA). Figure 7.2 shows an example of a smooth muscle cell during stretch. The position of the pipette tips was measured to obtain gauge length L and the displacement of the deflection pipette x. The force applied to the cell F was calculated by multiplying the displacement x with the spring constant of the deflection pipette k measured after each test. The elongation ΔL was calculated as the increment of L. The nominal stress was calculated by dividing force F with the original cross-sectional area, A_0, which is obtained from the diameter before the stretch assuming circular cross section, *i.e.*, $A_0 = \pi (D_0/2)^2$. The nominal strain was obtained by normalizing the elongation ΔL with the original gauge length L_0.

Mechanical properties of the cells can be evaluated with tension-elongation and nominal stress-nominal strain curves. Slope of the tension-elongation curves is used to evaluate stiffness, while that of stress-strain curves can be used for elastic modulus. Two different elastic moduli can be obtained from the nominal stress-nominal strain curves. An overall elastic modulus E_{all} is obtained by fitting a

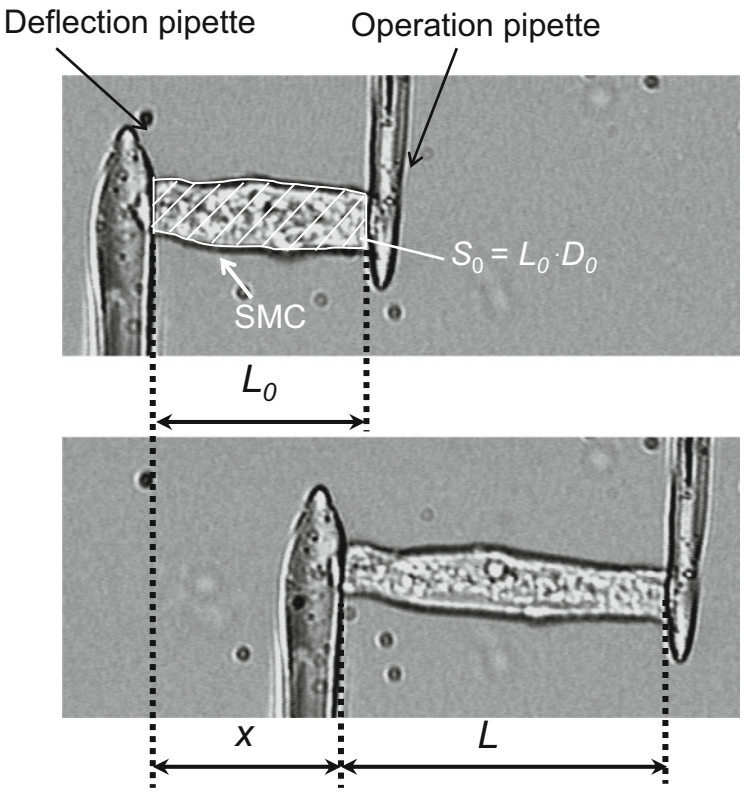

Fig. 7.2 Measurement of deformation of a freshly isolated aortic smooth muscle cell during tensile test. Mean diameter D_0 was calculated from the hatched area S_0 divided by the gauge length L_0

straight line from the origin to the entire segment of each curve. An initial elastic modulus E_{init} is obtained by fitting a straight line from the origin to the low strain region (nominal strain < 0.2) of each curve.

7.2 Tensile Properties of Smooth Muscle Cells: Relaxed vs Contractile State

7.2.1 Contraction and Relaxation of Vascular Smooth Muscle Cells

Vascular smooth muscle cells (VSMCs) contract in response to nervous, hormonal, and mechanical stimuli. Their contraction reduces vascular diameter especially at arteriolar level and thus plays vital role in controlling local blood flow. It has been pointed out that the characteristic impedance of the artery is maintained at minimum levels with the contraction of VSMCs (Cox 1975). It has also been suggested

that the artery wall might control its intramural stress distribution through smooth muscle contraction and relaxation (Matsumoto et al. 1996). Since the state of contraction of VSMCs (tonus) in a physiological condition lies between relaxed and fully contracted states, we need to know their mechanical properties under the both states. In this subsection, the mechanical properties of VSMCs obtained from rat thoracic aortas are introduced.

7.2.2 Isolation of Vascular Smooth Muscle Cells and Tensile Test

Rat aortic smooth muscle cells (RASMs) were isolated from aortic tissue by enzymatic digestion (Nagayama et al. 2006). Briefly, the descending thoracic aortas excised from male Wistar rats were placed in a physiological saline solution and loose connective tissue on their surface was removed. The aortas were placed in 3 ml of a Ca^{2+}-Mg^{2+}-free Hanks' balanced salt solution (HBSS, Gibco) at 37 °C containing 300U of collagenase type III (Worthington Biochemical Corp.) and 1.8U of elastase type I (Sigma), and agitated at about 1 Hz for 120–150 min to get cell suspension. The cell suspension was immediately dropped into a Petri dish filled with a Ca^{2+}-Mg^{2+}-free phosphate buffered saline (Nissui, Japan) to reduce the effect of enzymes. The Petri dish containing specimen cells was then set on the microscope stage whose temperature was controlled at 37 °C. A cell in the dish was held with the two pipettes by pressing the micropipettes coated with the urethane adhesive gently onto the cell. To omit cells that had already contracted, RASMs whose axial length was longer than 20 μm were used for the tensile test. The cell was then stretched by moving the pipette connected to the electric manipulator stepwise every 5 s with an increment of 1 μm until fracture or until the cell began slipping off from the pipette. The rate of the pipette movement was set to keep the strain rate in each cell within the range of 0.2–4 %/s, in which the elastic modulus did not change significantly with the strain rate in our system (Matsumoto et al. 2005).

7.2.3 Tensile Test Results

Figure 7.3 shows examples of the tensile properties of relaxed and contracted VSMCs isolated from rat thoracic aortas. A maximal contraction was induced with 10^{-5} M serotonin, and the initial normalized stiffness, i.e., initial elastic modulus, increased drastically from 14.8 ± 9.6 kPa (mean ± SEM, $n = 5$) to 88.1 ± 26.6 ($n = 4$) sixfold in response to contraction (Nagayama and Matsumoto 2004). Similar results were obtained for VSMCs isolated from rabbit thoracic aortas: 15.5 ± 6.9 kPa ($n = 6$) for relaxed cells and 156.4 ± 105.9 ($n = 8$) for maximally contracted cells (Matsumoto and Nagayama 2012). These results may indicate that the tension borne by the VSMCs in the aortic wall increases several times upon maximal contraction. In contrast, the contraction decreases

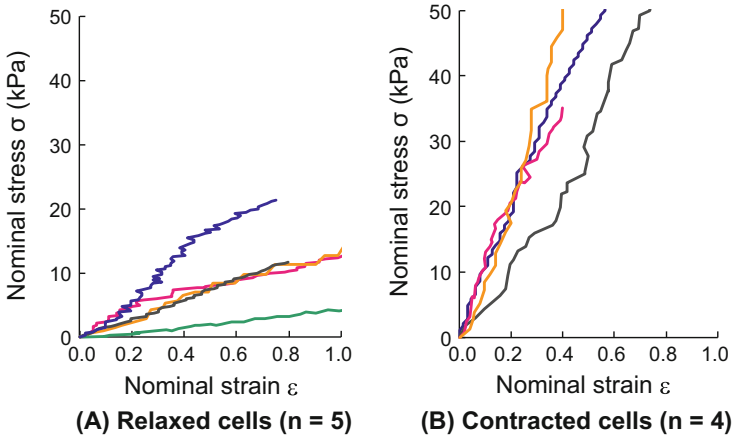

Fig. 7.3 Tensile properties of smooth muscle cells freshly isolated from rat thoracic aortas. Nominal stress-nominal strain curves of untreated cells (**a**) and of cells fully contracted with 10^{-5} M serotonin (**b**)

circumferential strain and stress applied to collagen and elastin. Taken together, the proportion of the stress borne by VSMCs may change significantly depending on the tonus of the VSMCs.

7.3 Tensile Properties of Smooth Muscle Cells: Anisotropy

7.3.1 Anisotropy of Smooth Muscle Cells

Vascular smooth muscle cells are spindle-shaped and aligned almost parallel to the circumferential direction in the arterial wall. Their intracellular contractile apparatus, i.e., stress fibers, run mostly parallel to their major axis and their contraction takes place in that direction. According to Deguchi et al. (2006), Young's modulus of the stress fibers is 1.45 MPa, *i.e.*, approximately two orders of magnitude higher than that of whole cells under relaxation. Thus, VSMCs might be much stiffer in the major axis direction than in minor. To check this hypothesis, the tensile properties of VSMCs freshly isolated from rat aortas were measured in their major and minor axes.

7.3.2 Protocol of the Experiment

RASMs were isolated from the thoracic aortas of male Wistar rats (8–14 weeks of age) as shown in Sect. 7.2.2. A cell in a dish was held with the two micropipettes coated with the urethane adhesive. When the cell was stretched along its major axis, each of the glass micropipettes was gently pressed down on each end of the cell.

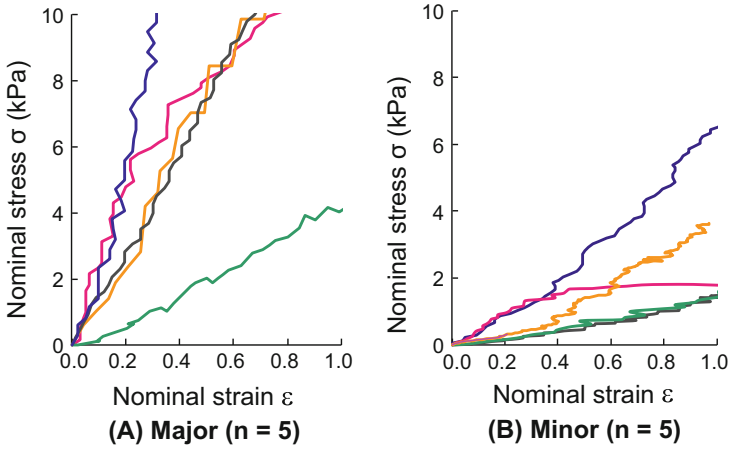

Fig. 7.4 Nonimal stress–nominal strain curves of the freshly isolated rat aortic smooth muscle cells stretched in their major (**a**) and minor (**b**) axis directions

The cell was held gently on both sides with the two pipettes when stretched in the minor axis direction. After waiting for about 5 min to make the adhesion between the cell and the pipettes firm, we stretched the cell stepwise by moving the operation pipette 1 μm every 5 s until fracture occurred, or until the cell began to slip off from the pipette.

7.3.3 Tensile Test Results

The normalized tension–nominal strain curves in major and minor axes are shown in Fig. 7.4. The relationship between the normalized tension and the nominal strain was relatively linear in the major and minor axis directions. The slopes in the major axis looked steeper than those in the minor axis. The initial elastic modulus E_{ini} of FSMCs was significantly higher in the major axis (14.8 ± 4.3 kPa, $n = 5$) than in the minor axis (2.8 ± 1.0 kPa, $n = 5$), indicating that freshly isolated SMCs are anisotropic.

7.4 Viscoelastic Properties of Smooth Muscle Cells

7.4.1 Importance of Consideration for Viscoelasticity of Smooth Muscle Cells

It is well known that intestinal smooth muscle cells are highly viscoelastic. Their viscoelastic response is not only passive but also active, *i.e.*, their response is dependent on extracellular environment such as temperature and drugs (Price et al. 1979). Vascular smooth muscle cells are no exception. Since artery wall is

subjected to cyclic deformation during heartbeat, VSMCs may experience loads higher than that expected from elastic analysis. Thus, consideration of viscoelastic properties is important. In this subsection, tension relaxation test, one of the most simple viscoelastic tests, is applied to RASMs (Nagayama et al. 2007).

7.4.2 Tensile Tester for Tension Relaxation

When measuring tension relaxation response, specimen length must be kept constant. Since tension applied to the specimen is measured by the deformation of the deflection pipette in the conventional micro tensile testers, specimen length changes in response to tension relaxation. To overcome this problem, the position of micropipette should be controlled precisely. A micro tensile tester with such capability is shown in Fig. 7.5a (Nagayama et al. 2007). To control pipette position precisely, a pantagraph-type piezo actuator has been added to a conventional tensile tester. The tips of the glass micropipettes were painted black to enhance image binarization. The position of the micropipette tips was tracked using an image processor (Percept Scope, C8840, Hamamatsu Photonics, Hamamatsu, Japan) to obtain the distance between the pipettes (Fig. 7.5b). The specimen length was maintained constant by a position feedback mechanism in which the distance between the micropipettes was controlled by changing electric voltage applied to the piezo ceramics. Tension applied to the specimen was calculated from the deformation of the deflectable pipette that was derived from the position of the pipette tip and the pipette root, which was obtained from the deformation of the piezo ceramics measured by the strain gauge attached on the ceramics.

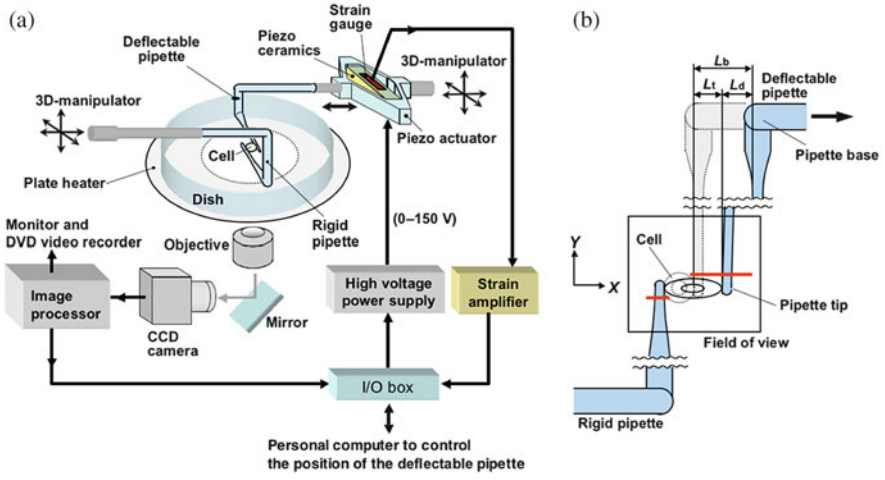

Fig. 7.5 Schematic diagram of the micro tensile tester with feed-back control (**a**), and the details of its test section (**b**). *Red lines* in the field of view indicate the binarized regions to track the outline edge of the pipettes with the image processor (Nagayama et al. 2007)

7.4.3 Tension Relaxation Test

RASMs were obtained as stated in Sect. 7.2.2 and cultured in DMEM supplemented with 10 % fetal bovine serum up to passage 3. Untreated cultured cells (SMCs) and cultured SMCs whose actin filaments (AFs) were disrupted with cytochalasin D (SMCs-CD) were used to know the effects of AFs on the viscoelastic properties of cells. Either type of cell was mounted on the tensile tester, stretched by 75 %, and its length was kept constant for 20–30 min using the position feedback control. Tension relaxation response was modeled using a 4-parameter Maxwell model (Fig. 7.6 insert) consisting of two parallel Maxwell chains, a serial combination of an elastic component with elastic parameter K^* and a dashpot with viscous parameter V^*. By assuming a step input of strain $\varepsilon(0)$, the tension normalized by the initial cross sectional area of the specimen $T^*(t)$ was expressed by the following equation:

$$T^*(t) = \left\{ K_0^* \cdot \exp\left(-\frac{t}{\tau_0}\right) + K_1^* \cdot \exp\left(-\frac{t}{\tau_1}\right) \right\} \cdot \varepsilon(0), \tag{1}$$

where the relaxation time constant τ_0 equals V_0^*/K_0^*, τ_1 equals V_1^*/K_1^*, and $\varepsilon(0)$ represents the strain at the beginning of the tension relaxation. Model parameters were determined by minimizing errors between the theoretical and experimental curves for each cell.

Figure 7.6 shows the typical examples of the relaxation responses of SMCs and SMCs-CD fitted with 4-parameter Maxwell model. Fitting of the relaxation curves obtained with the 4-parameter Maxwell model was satisfactory for both cells ($R^2 > 0.95$). Some fluctuation in tension was observed in the SMCs, while the curves for SMCs-CD were relatively smooth. The viscoelastic parameters of

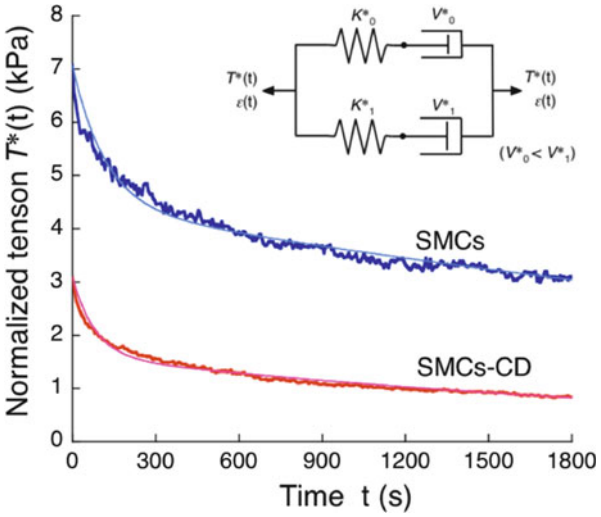

Fig. 7.6 Typical examples of the stress relaxation curves for SMCs and SMCs-CD fitted by the 4-parameter Maxwell model. *Thick lines* and *thin lines* indicate experiment data and approximate curves, respectively (Nagayama et al. 2007)

Table 7.1 Summary of the viscoelastic parameters of SMCs and SMCs-CD (mean ± SEM) (Nagayama et al. 2007)

Group	n	K_0* (kPa)	K_1* (kPa)	V_0* (kPa·s)	V_1* (kPa·s)	τ_0 (s)	τ_1 (s)
SMCs	11	6.45 ± 1.60	5.69 ± 1.01	372 ± 93	20510 ± 4330	57.1 ± 9.0	3620 ± 470
SMCs-CD	6	2.49 ± 0.56$^{\#}$	2.39 ± 0.43$^{\#}$	109 ± 24$^{\#}$	4740 ± 700$^{\#}$	46.7 ± 9.7	1820 ± 230$^{\#}$

K_0* and K_1*, elastic parameters; V_0* and V_1*, viscous parameters; τ_0 and τ_1, relaxation time constants ($= V_n$*/K_n*, $n = 1, 2$). $^{\#}P < 0.05$

SMCs and SMCs-CD were compared in Table 7.1. The elastic parameters of SMCs-CD were one-half of those of SMCs. The viscous parameters also decreased following AF disruption, with the decrease being larger for V_1* than V_0*. These changes in the elastic and viscous parameters caused the change in the relaxation time constant ($\tau = V^*/K^*$): The τ_0 did not change significantly with AF disruption, while τ_1 significantly decreased following the disruption.

These results indicate that AFs have crucial roles not only in elastic properties of VSMCs but also in their viscous properties, especially in the slow response of stress relaxation. AFs also have significant effects on the fluctuation in tension during stress relaxation of SMCs. Viscoelastic response of VSMCs is not passive but active response of the cells.

7.5 Isolation and Measurement of Tensile Properties of Elastic Lamina

7.5.1 Mechanical Behavior of Elastic Lamina in the Vascular Wall

Elastic lamina (EL) is a several μm-thick layer of elastic tissue mainly composed of elastin and forms boundary of intima and the media (internal EL) and of media and adventitia (external EL) of the arteries. ELs are abundant on elastic arteries, for their media has concentric layers of elastic laminas. Elastin is the most linearly elastic materials known (Fung 1981) and plays pivotal roles in maintaining elastic properties of blood vessel wall. It is well known that EL is corrugated in the section perpendicular to the axial direction in no load state, while it becomes straight in a physiological state. Measurement of the mechanical properties of the EL is important in elucidating mechanical interaction between smooth muscle cells and surrounding matrix.

7.5.2 Specimen Preparation

Ten-μm-thick sections perpendicular to the axial direction were obtained from porcine thoracic aortas with a cryotome. An EL was excised from the surrounding tissues by a micro dissector (5190, Eppendorf, Germany) and remaining tissues were removed by enzymatic digestion with purified collagenase (Worthington

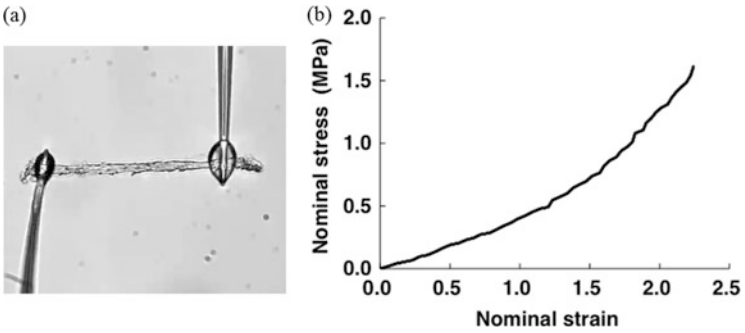

Fig. 7.7 Typical example of tensile test of elastic lamina obtained from the aorta. (**a**) Typical image of tensile test. (**b**) An example of stress-strain curve

Biochemical, USA). Shape change of the EL during isolation was observed. Tensile properties of the isolated ELs were then measured as described in Sect. 7.1. Specimens were stretched by 5 μm every 3 s to obtain tension-stretch ratio curves. Width and thickness of each EL were measured under a microscope before the tensile test to convert tension to stress.

7.5.3 Tensile Test Results

ELs became almost straightened following isolation process, indicating that the corrugation of the ELs in the unloaded aortic wall is mainly due to compressive residual stress in the ELs caused by surrounding tissues (Matsumoto et al. 2004). Nominal stress–stretch ratio relation of the ELs was almost linear up to nominal strain of 1.0 with Young's modulus of 440 kPa (Fig. 7.7). These results indicate that tension applied to the ELs in a physiological state is dependent on the degree of the corrugation. Since there is wide variation of the corrugation in the unloaded aortic walls, physiological tension borne by the ELs might also have a wide variation.

7.6 Tensile Properties of Fibrous Collagen in the Aorta

7.6.1 Mechanical Behavior of Collagen in the Vascular Wall

As described in the beginning of this section, collagen is the stiffest material in the vascular wall, and it plays important roles in the nonlinear (strain-hardening) mechanical properties of the vascular walls and in preventing overstretch of the wall. Mechanical properties of collagen fibers have been obtained mainly by uniaxial tensile test for collagen fibrils, fibers, and fascicles obtained from tendons. Stress-strain curves of the rabbit patellar tendon showed the linear relationship and tangent elastic modulus of 732 ± 200 MPa (Yamamoto et al. 1999). It should be noted that mechanical properties of collagenous tissues obtained from rabbit tendon

were dependent on their size, *i.e.*, specimen diameter (D). Young's modulus of rabbit patellar tendon fascicles ($D \sim 300$ μm) was reported to be 216 ± 68 MPa (Yamamoto et al. 1999), while that of fibrils ($D = 1.01 \pm 0.06$ μm) was 54.3 ± 25.1 MPa (Miyazaki and Hayashi 1999). Yamamoto et al. (1999) stated that this difference might be attributable to such interactions as frictional force between collagen fascicles as well as between collagen fascicles and ground substance. Young's modulus of collagen obtained from other parts of the body ranges from several hundreds of MPa to ~1 GPa: the maximum tangent elastic modulus of rat tail tendon fascicles was 1–2 GPa (Svendsen and Thomson 1984), tangent elastic modulus of mouse tail tendon ($D \sim 100$ μm) 423.5 ± 76.6 MPa, and sea cucumber collagen fibrils ($D = 0.21$–0.45 μm) 470 ± 410 MPa (Shen et al. 2010).

7.6.2 Preparation of Collagen Fiber Specimens

To obtain the mechanical properties of collagen fibers in the aorta, other main constituents such as smooth muscle cells and elastin should be removed. Fibrous collagen in the aorta was obtained as follows: (1) thoracic aortas were excised and its adventitia and loose connective tissues on adventitial side were trimmed off; (2) the specimens were incubated in 68.5 U/ml of highly purified elastase (ES438, EPC, USA) for 2 h; (3) and they were cut into fibrous collagens of a few micrometers in diameter and ~100 μm in length by shaking the container containing the specimen. These specimens were then glued on two glass pipettes with urethane adhesive (Sista M5250, Henkel, Germany) to perform tensile test as stated in Sect. 7.4.1 (Fig. 7.8a). Stress-strain curve was obtained assuming that the specimen had a circular cross section.

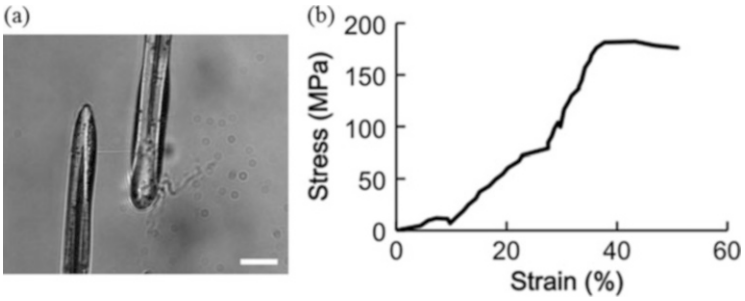

Fig. 7.8 Typical example of tensile test of fibrous collagen obtained from the aorta. (**a**) Typical image of tensile test. Scale bar = 30 μm. (**b**) An example of stress-strain curve of fibrous collagen

7.6.3 Tensile Test Results

An example of stress-strain curve of a collagen fiber obtained from a porcine thoracic aorta was shown in Fig. 7.8b. Calculated Young's modulus of collagen fibers in the aorta was ~500 MPa, which was comparable to that of collagen fibers obtained from other tissues. The curve seemed to have multiple linear regions. This may indicate that the specimen was composed of multiple thinner fibers with different slack length. Similar phenomena were observed in the collagen fibrils obtained from the sea cucumber (Shen et al. 2010). Although their elastic modulus is dependent on specimen diameter, collagen fibers are still the stiffest material in the artery wall at a microscopic level. Roughly speaking, collagen fibers are 1000 times stiffer than the ELs and 10,000 times stiffer than the VSMCs. Collagen fibers may play important roles on intramural force transmission, although they are not abundant in the media of the arteries.

References

Cox R (1975) Pressure dependence of the mechanical properties of arteries in vivo. Am J Physiol 229:1371–1375

Deguchi S, Ohashi T, Sato M (2006) Tensile properties of single stress fibers isolated from cultured vascular smooth muscle cells. J Biomech 39:2603–2610

Fung YC (1981) Bio-viscoelastic solids. In: Biomechanics. Springer, New York, pp 196–214

Hochmuth R (2000) Micropipette aspiration of living cells. J Biomech 33:15–22

Hoh J, Schoenenberger C (1994) Surface morphology and mechanical properties of MDCK monolayers by atomic force microscopy. J Cell Sci 107:1105–1114

Matsumoto T, Nagayama K (2012) Tensile properties of vascular smooth muscle cells: bridging vascular and cellular biomechanics (review). J Biomech 45:745–755

Matsumoto T, Tsuchida M, Sato M (1996) Change in intramural strain distribution in rat aorta due to smooth muscle contraction and relaxation. Am J Physiol Heart Circ Physiol 271:H1711–H1716

Matsumoto T, Goto T, Furukawa T, Sato M (2004) Residual stress and strain in the lamellar unit of the porcine aorta: experiment and analysis. J Biomech 37:807–815

Matsumoto T, Sato J, Yamamoto M, Sato M (2005) Development of a novel micro tensile tester for single isolated cells and its application to viscoelastic analysis of aortic smooth muscle cells. In: Biomechanics at micro- and nanoscale levels, vol I. World Scientific, Singapore, pp 16–25

Miyazaki H, Hayashi K (1999) Tensile tests of collagen fibers obtained from the rabbit patellar tendon. Biomed Microdevices 2:151–157

Nagayama K, Matsumoto T (2004) Mechanical Anisotropy of Rat Aortic Smooth Muscle Cells Decreases with Their Contraction: Possible effect of actin filament orientation. JSME Int J Ser C 47:985–991

Nagayama K, Matsumoto T (2008) Contribution of actin filaments and microtubules to quasi-in situ tensile properties and internal force balance of cultured smooth muscle cells on a substrate. Am J Physiol Cell Physiol 295:C1569–C1578

Nagayama K, Nagano Y, Sato M, Matsumoto T (2006) Effect of actin filament distribution on tensile properties of smooth muscle cells obtained from rat thoracic aortas. J Biomech 39:293–301

Nagayama K, Yanagihara S, Matsumoto T (2007) Actin filaments affect on not only elasticity but also late viscous response in stress relaxation of single isolated aortic smooth muscle cells (Possible effect of active reorganization of actin filaments). J Biomech Sci Eng 2:93–104

Price JM, Patitucci PJ, Fung YC (1979) Mechanical properties of resting taenia coli smooth muscle. Am J Physiol Cell Physiol 236(5):C211–C220

Sato M, Nagayama K, Kataoka N, Sasaki M, Hane K (2000) Local mechanical properties measured by atomic force microscopy for cultured bovine endothelial cells exposed to shear stress. J Biomech 33:127–135

Shen ZL, Dodge MR, Kahn H, Ballarini R, Eppell SJ (2010) In vitro fracture testing of submicron diameter collagen fibril specimens. Biophys J 99:1986–1995

Svendsen KH, Thomson G (1984) A new clamping and stretching procedure for determination of collagen fiber stiffness and strength relations upon maturation. J Biomech 17:225–229

Wang N, Butler J, Ingber D (1993) Mechanotransduction across the cell surface and through the cytoskeleton. Science 260:1124–1127

Warshaw D, Fay F (1983) Cross-bridge elasticity in single smooth muscle cells. J Gen Physiol 82:157–199

Wolinsky H, Glagov S (1967) A lamellar unit of aortic medial structure and function in mammals. Circ Res 20:99–111

Yamamoto E, Hayashi K, Yamamoto N (1999) Mechanical properties of collagen fascicles from the rabbit patellar tendon. J Biomech Eng 121:124–131